8

Bipolar Transistor

CHAPTER OBJECTIVES

This chapter introduces the bipolar junction transistor (BJT) operation and then presents the theory of the bipolar transistor I-V characteristics, current gain, and output conductance. High-level injection and heavy doping induced band narrowing are introduced. SiGe transistor, transit time, and cutoff frequency are explained. Several bipolar transistor models are introduced, i.e., Ebers–Moll model, small-signal model, and charge control model. Each model has its own areas of applications.

The **bipolar junction transistor** or **BJT** was invented in 1948 at Bell Telephone Laboratories, New Jersey, USA. It was the first mass produced transistor, ahead of the MOS field-effect transistor (MOSFET) by a decade. After the introduction of metal-oxide-semiconductor (MOS) ICs around 1968, the high-density and low-power advantages of the MOS technology steadily eroded the BJT's early dominance. BJTs are still preferred in some high-frequency and analog applications because of their high speed, low noise, and high output power advantages such as in some cell phone amplifier circuits. When they are used, a small number of BJTs are integrated into a high-density complementary MOS (CMOS) chip. Integration of BJT and CMOS is known as the **BiCMOS technology**.

The term **bipolar** refers to the fact that both electrons and holes are involved in the operation of a BJT. In fact, minority carrier diffusion plays the leading role just as in the PN junction diode. The word **junction** refers to the fact that PN junctions are critical to the operation of the BJT. BJTs are also simply known as **bipolar transistors**.

8.1 ● INTRODUCTION TO THE BJT ●

A BJT is made of a heavily doped **emitter** (see Fig. 8–1a), a P-type **base**, and an N-type **collector**. This device is an **NPN** BJT. (A **PNP** BJT would have a P^+ emitter, N-type base, and P-type collector.) NPN transistors exhibit higher transconductance and

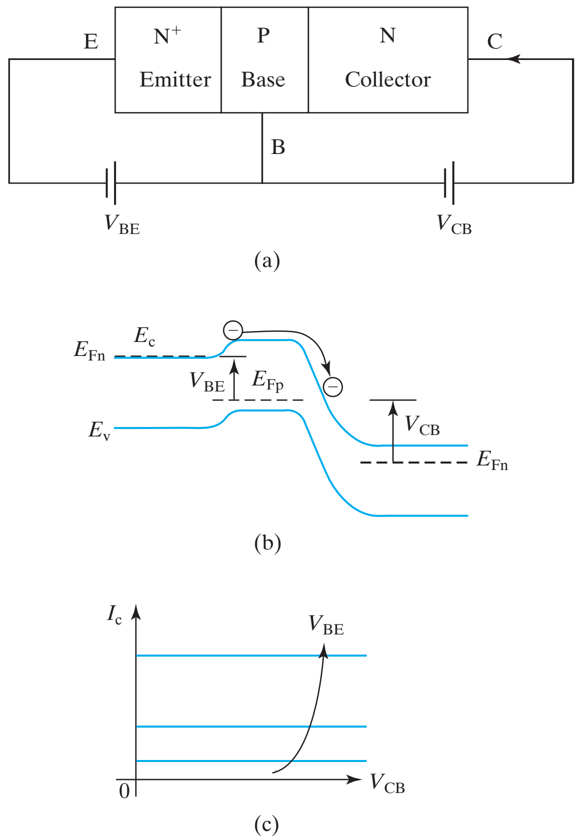

FIGURE 8–1 (a) Schematic NPN BJT and normal voltage polarities; (b) electron injection from emitter into base produces and determines I_C; and (c) I_C is basically determined by V_{BE} and is insensitive to V_{CB}.

speed than PNP transistors because the electron mobility is larger than the hole mobility. BJTs are almost exclusively of the NPN type since high performance is BJTs' competitive edge over MOSFETs.

Figure 8–1b shows that when the base–emitter junction is forward biased, electrons are injected into the more lightly doped base. They diffuse across the base to the reverse-biased base–collector junction (edge of the depletion layer) and get swept into the collector. This produces a **collector current**, I_C. I_C is independent of V_{CB} as long as V_{CB} is a reverse bias (or a small forward bias, as explained in Section 8.6). Rather, I_C is determined by the rate of electron injection from the emitter into the base, i.e., determined by V_{BE}. You may recall from the PN diode theory that the rate of injection is proportional to $e^{qV_{BE}/kT}$. These facts are obvious in Fig. 8–1c.

Figure 8–2a shows that the emitter is often connected to ground. (The emitter and collector are the equivalents of source and drain of a MOSFET. The base is the equivalent of the gate.) Therefore, the I_C curve is usually plotted against V_{CE} as shown in Fig. 8–2b. For V_{CE} higher than about 0.3 V, Fig. 8–2b is identical to Fig. 8–1c but with a shift to the right because $V_{CE} = V_{CB} + V_{BE}$. Below $V_{CE} \approx 0.3$ V,

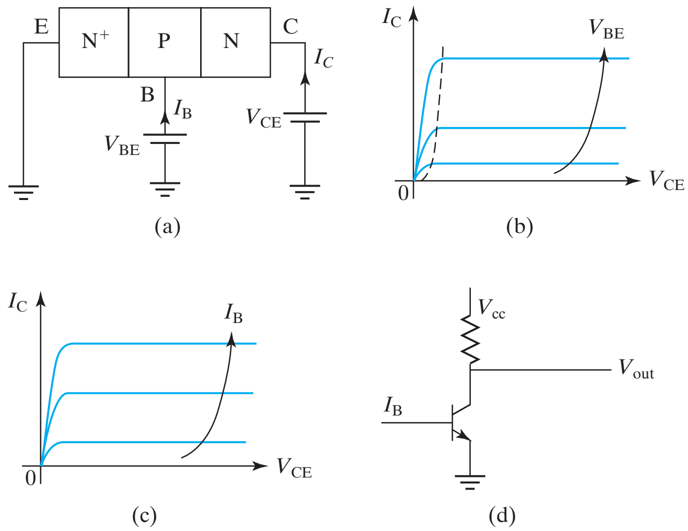

FIGURE 8–2 (a) Common-emitter convention; (b) I_C vs. V_{CE}; (c) I_B may be used as the parameter instead of V_{BE}; and (d) circuit symbol of an NPN BJT and an inverter circuit.

the base–collector junction is strongly forward biased and I_C decreases as explained in Section 8.6. Because of the parasitic IR drops, it is difficult to accurately ascertain the true base–emitter junction voltage. For this reason, the easily measurable base current, I_B, is commonly used as the variable parameter in lieu of V_{BE} (as shown in Fig. 8–2c). We will see later that I_C is proportional to I_B.

8.2 • COLLECTOR CURRENT •

The collector current is the output current of a BJT. Applying the electron diffusion equation [Eq. (4.7.7)] to the base region,

$$\frac{d^2 n'}{dx^2} = \frac{n'}{L_B^2} \tag{8.2.1}$$

$$L_B \equiv \sqrt{\tau_B D_B} \tag{8.2.2}$$

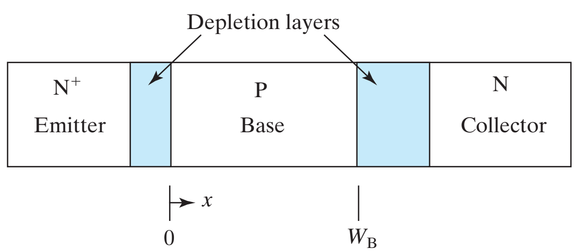

FIGURE 8–3 $x = 0$ is the edge of the BE junction depletion layer. W_B is the width of the base neutral region.

τ_B and D_B are the recombination lifetime and the minority carrier (electron) diffusion constant in the base, respectively. The boundary conditions are [Eq. (4.6.3)]

$$n'(0) = n_{B0}(e^{qV_{BE}/kT} - 1) \tag{8.2.3}$$

$$n'(W_B) = n_{B0}(e^{qV_{BC}/kT} - 1) \approx -n_{B0} \approx 0 \tag{8.2.4}$$

where $n_{B0} = n_i^2/N_B$, and N_B is the base doping concentration. V_{BE} is normally a forward bias (positive value) and V_{BC} is a reverse bias (negative value). The solution of Eq. (8.2.1) is

$$n'(x) = n_{B0}(e^{qV_{BE}/kT} - 1)\frac{\sinh\left(\dfrac{W_B - x}{L_B}\right)}{\sinh(W_B/L_B)} \tag{8.2.5}$$

Equation (8.2.5) is plotted in Fig. 8–4.

Modern BJTs have base widths of about 0.1 μm. This is much smaller than the typical diffusion length of tens of microns (see Example 4–4 in Section 4.8). In the case of $W_B << L_B$, Eq. (8.2.5) reduces to a straight line as shown in Fig. 8–4.

$$\boxed{\begin{aligned} n'(x) &= n'(0)(1 - x/W_B) \\ &= \frac{n_{iB}^2}{N_B}(e^{qV_{BE}/kT} - 1)\left(1 - \frac{x}{W_B}\right) \end{aligned}} \tag{8.2.6}$$

n_{iB} is the intrinsic carrier concentration of the base material. The subscript, B, is added to n_i because the base may be made of a different semiconductor (such as SiGe alloy, which has a smaller band gap and therefore a larger n_i than the emitter and collector material).

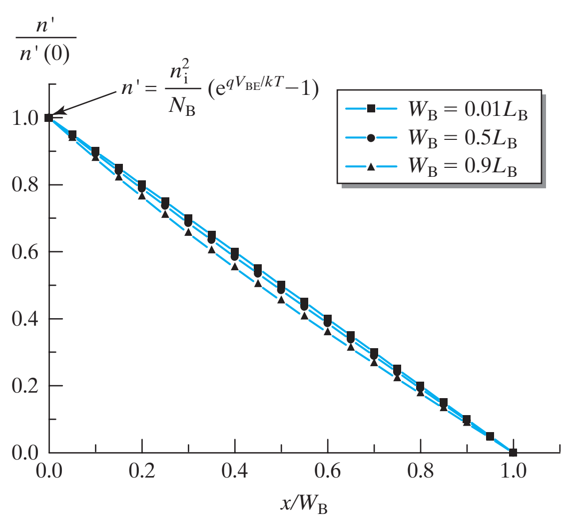

FIGURE 8–4 When $W_B << L_B$, the excess minority carrier concentration in the base is approximately a linear function of x.

As explained in the PN diode analysis, the minority-carrier current is dominated by the diffusion current. The sign of I_C is defined in Fig. 8–2a and is positive.

$$
\begin{aligned}
I_C &= \left|A_E q D_B \frac{dn}{dx}\right| = A_E q D_B \frac{n'(0)}{W_B} \\
&= A_E q \frac{D_B}{W_B}\frac{n_{iB}^2}{N_B}(e^{qV_{BE}/kT} - 1)
\end{aligned}
\tag{8.2.7}
$$

A_E is the area of the BJT, specifically the emitter area. Notice the similarity between Eq. (8.2.7) and the PN diode IV relation [Eq. (4.9.4)]. Both are proportional to $(e^{qV/kT} - 1)$ and to Dn_i^2/N. In fact, the only difference is that dn'/dx has produced the $1/W_B$ term in Eq. (8.2.7) due to the linear n' profile. Equation (8.2.7) can be condensed to

$$
I_C = I_S(e^{qV_{BE}/kT} - 1) \tag{8.2.8}
$$

where I_S is the saturation current. Equation (8.2.7) can be rewritten as

$$
I_C = A_E \frac{qn_i^2}{G_B}(e^{qV_{BE}/kT} - 1) \tag{8.2.9}
$$

In the special case of Eq. (8.2.7)

$$
G_B = \frac{n_i^2}{n_{iB}^2}\frac{N_B}{D_B}W_B = \frac{n_i^2}{n_{iB}^2}\frac{p}{D_B}W_B \tag{8.2.10}
$$

where p is the majority carrier concentration in the base. It can be shown that Eq. (8.2.9) is valid even for nonuniform base and high-level injection condition if G_b is generalized to [1]

$$
G_B \equiv \int_0^{W_B} \frac{n_i^2}{n_{iB}^2}\frac{p}{D_B}dx \tag{8.2.11}
$$

G_B has the unusual dimension of s/cm^4 and is known as the **base Gummel number**. In the special case of $n_{iB} = n_i$, D_B is a constant, and $p(x) = N_B(x)$ (low-level injection),

$$
G_B = \frac{1}{D_B}\int_0^{W_B} N_B(x)dx = \frac{1}{D_B} \times \text{base dopant atoms per unit area} \tag{8.2.12}
$$

Equation (8.2.12) illustrates that the base Gummel number is basically proportional to the base dopant density per area. The higher the base dopant density is, the lower the I_C will be for a given V_{BE} as given in Eq. (8.2.9).

The concept of a Gummel number simplifies the I_C model because it [Eq. (8.2.11)] contains all the subtleties of transistor design that affect I_C: changing base material through $n_{iB}(x)$, nonconstant D_B, nonuniform base dopant concentration through $p(x) = N_B(x)$, and even the **high-level injection** condition (see Sec. 8.2.1), where $p > N_B$. Although many factors affect G_B, G_B can be easily determined from the **Gummel plot** shown in Fig. 8–5. The (inverse) slope of the

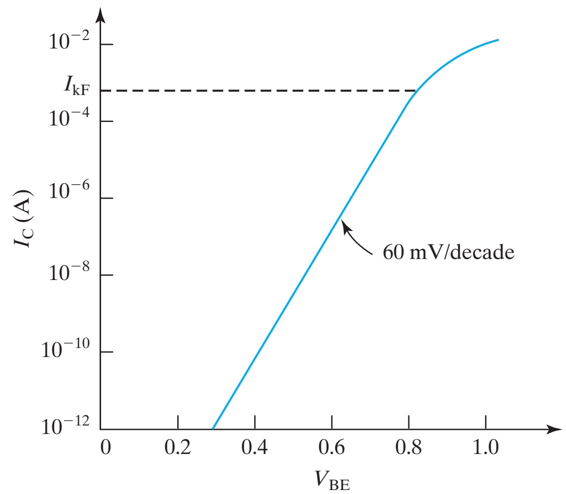

FIGURE 8–5 I_C is an exponential function of V_{BE}.

straight line in Fig. 8–5 can be described as 60 mV per decade. The extrapolated intercept of the straight line and $V_{BE} = 0$ yields I_S [Eq. (8.2.8)]. G_B is equal to $A_E q n_i^2$ divided by the intercept.

8.2.1 High-Level Injection Effect

The decrease in the slope of the curve in Fig. 8–5 at high I_C is called the **high-level injection effect**. At large V_{BE}, n' in Eq. (8.2.3) can become larger than the base doping concentration N_B

$$n' = p' \gg N_B \tag{8.2.13}$$

The first part of Eq. (8.2.13) is simply Eq. (2.6.2) or charge neutrality. The condition of Eq. (8.2.13) is called **high-level injection**. A consequence of Eq. (8.2.13) is that in the base

$$n \approx p \tag{8.2.14}$$

From Eqs. (8.2.14) and (4.9.6)

$$n \approx p \approx n_i e^{qV_{BE}/2kT} \tag{8.2.15}$$

Equations (8.2.15) and (8.2.11) yield

$$G_B \propto n_i e^{qV_{BE}/2kT} \tag{8.2.16}$$

Equations (8.2.16) and (8.2.9) yield

$$I_c \propto n_i e^{qV_{BE}/2kT} \tag{8.2.17}$$

Therefore, at high V_{BE} or high I_c, $I_c \propto e^{qV_{BE}/2kT}$ and the (inverse) slope in Fig. 8–5 becomes 120 mV/decade. I_{kF}, the **knee current**, is the current at which the slope changes. It is a useful parameter in the BJT model for circuit simulation. The IR drop in the parasitic resistance significantly increases V_{BE} at very high I_C and further flattens the curve.

8.3 ● BASE CURRENT ●

Whenever the base–emitter junction is forward biased, some holes are injected from the P-type base into the N$^+$ emitter. These holes are provided by the base current, I_B.[1] I_B is an undesirable but inevitable side effect of producing I_C by forward biasing the BE junction. The analysis of I_B, the base to emitter injection current, is a perfect parallel of the I_C analysis. Figure 8–6b illustrates the mirror equivalence. At an ideal ohmic contact such as the contact of the emitter, the equilibrium condition holds and $p' = 0$ similar to Eq. (8.2.4). Analogous to Eq. (8.2.9), the base current can be expressed as

$$I_B = A_E \frac{qn_i^2}{G_E}(e^{qV_{BE}/kT} - 1) \tag{8.3.1}$$

$$G_E = \int_0^{W_E} \frac{n_i^2}{n_{iE}^2} \frac{n}{D_E} dx \tag{8.3.2}$$

G_E is the **emitter Gummel number**. As an exercise, please verify that in the special case of a uniform emitter, where n_{iE}, N_E (emitter doping concentration) and D_E are not functions of x,

$$I_B = A_E q \frac{D_E n_{iE}^2}{W_E N_E}(e^{qV_{BE}/kT} - 1) \tag{8.3.3}$$

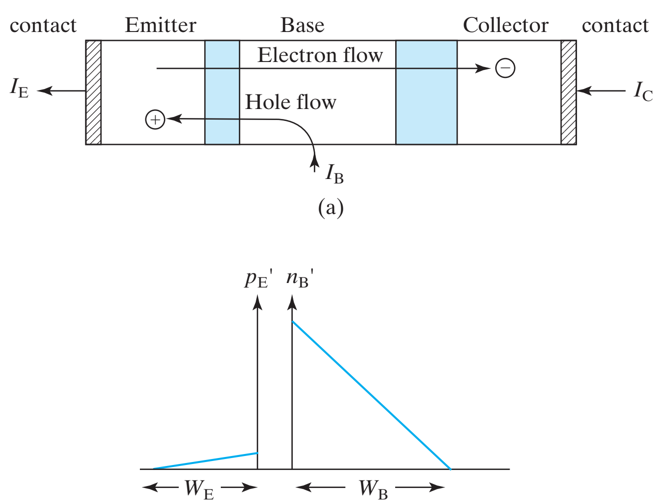

FIGURE 8–6 (a) Schematic of electron and hole flow paths in BJT; (b) hole injection into emitter closely parallels electron injection into base.[2]

[1] In older transistors with VERY long bases, I_B also supplies holes at a significant rate for recombination in the base. Recombination is negligible in the narrow base of a typical modern BJT.

[2] A good metal–semiconductor ohmic contact (at the end of the emitter) is an excellent source and sink of carriers. Therefore, the excess carrier concentration is assumed to be zero.

8.4 • CURRENT GAIN •

Perhaps the most important DC parameter of a BJT is its **common-emitter current gain**, β_F.

$$\boxed{\beta_F \equiv \frac{I_C}{I_B}} \tag{8.4.1}$$

Another current ratio, the **common-base current gain,** is defined by

$$I_C = \alpha_F I_E \tag{8.4.2}$$

$$\alpha_F \equiv \frac{I_C}{I_E} = \frac{I_C}{I_B + I_C} = \frac{I_C/I_B}{1 + I_C/I_B} = \frac{\beta_F}{1 + \beta_F} \tag{8.4.3}$$

α_F is typically very close to unity, such as 0.99, because β_F is large. From Eq. (8.4.3), it can be shown that

$$\beta_F = \frac{\alpha_F}{1 - \alpha_F} \tag{8.4.4}$$

I_B is a load on the input signal source, an undesirable side effect of forward biasing the BE junction. I_B should be minimized (i.e., β_F should be maximized). Dividing Eq. (8.2.9) by Eq (8.3.1),

$$\boxed{\beta_F = \frac{G_E}{G_B}} = \frac{D_B W_E N_E n_{iB}^2}{D_E W_B N_B n_{iE}^2} \tag{8.4.5}$$

A typical good β_F is 100. D and W in Eq. (8.4.5) cannot be changed very much. The most obvious way to achieve a high β_F, according to Eq. (8.4.5), is to use a large N_E and a small N_B. A small N_B, however, would introduce too large a base resistance, which degrades the BJT's ability to operate at high current and high frequencies. Typically, N_B is around 10^{18} cm^{-3}.

An emitter is said to be efficient if the emitter current is mostly the useful electron current injected into the base with little useless hole current (the base current). The **emitter efficiency** is defined as

$$\gamma_E = \frac{I_E - I_B}{I_E} = \frac{I_C}{I_C + I_B} = \frac{1}{1 + G_B/G_E} \tag{8.4.6}$$

EXAMPLE 8–1 Current Gain

A BJT has $I_C = 1$ mA and $I_B = 10$ µA. What are I_E, β_F, and α_F?

$$I_E = I_C + I_B = 1\,\text{mA} + 10\,\mu\text{A} = 1.01\,\text{mA}$$

$$\beta_F = \frac{I_C}{I_B} = \frac{1\,\text{mA}}{10\,\mu\text{A}} = 100$$

$$\alpha_F = \frac{I_C}{I_E} = \frac{1\,\text{mA}}{1.01\,\text{mA}} = 0.9901$$

SOLUTION:

Using this example, we can confirm Eqs. (8.4.3) and (8.4.4).

$$\frac{\beta_F}{1+\beta_F} = \frac{100}{101} = 0.9901 = \alpha_F$$

$$\frac{\alpha_F}{1-\alpha_F} = \frac{0.9901}{0.0099} = 100 = \beta_F$$

8.4.1 Emitter Band Gap Narrowing

To raise β_F, N_E is typically made larger than 10^{20} cm^{-3}. Unfortunately, when N_E is very large, n_{iE}^2 becomes larger than n_i^2. This is called the **heavy doping effect**. Recall Eq. (1.8.12)

$$n_i^2 = N_c N_v e^{-E_g/kT} \tag{8.4.7}$$

Heavy doping can modify the Si crystal sufficiently to reduce E_g and cause n_i^2 to increase significantly.[3] Therefore, the heavy doping effect is also known as **band gap narrowing**.

$$n_{iE}^2 = n_i^2 e^{\Delta E_{gE}/kT} \tag{8.4.8}$$

ΔE_{gE} is the narrowing of the emitter band gap relative to lightly doped Si and is negligible for $N_E < 10^{18}$ cm^{-3}, 50 meV at 10^{19} cm^{-3}, 95 meV cm^{-3} at 10^{20} cm^{-3}, and 140 meV at 10^{21} cm^{-3} [2].

8.4.2 Narrow Band-Gap Base and Heterojunction BJT

To further elevate β_F, we can raise n_{iB} by using a base material that has a smaller band gap than the emitter material. $Si_{1-\eta}Ge_\eta$ is an excellent base material candidate for an Si emitter. With $\eta = 0.2$, E_{gB} is reduced by 0.1 eV. In an SiGe BJT, the base is made of high-quality P-type epitaxial SiGe. In practice, η is graded such that $\eta = 0$ at the emitter end of the base and 0.2 at the drain end to create a built-in field that improves the speed of the BJT (see Section 8.7.2).

Because the emitter and base junction is made of two different semiconductors, the device is known as a **heterojunction bipolar transistor** or **HBT**. HBTs made of InP emitter ($E_g = 1.35$ eV) and InGaAs base ($E_g = 0.68$ eV) and GaAlAs emitter with GaAs base are other examples of well-studied HBTs. The ternary semiconductors are used to achieve lattice constant matching at the heterojunction (see Section 4.13.1).

[3] Heavy doping also affects n_i by altering N_c and N_v in a complex manner. It is customary to lump all these effects into an effective narrowing of the band gap.

EXAMPLE 8–2 Emitter Band-Gap Narrowing and SiGe Base

Assuming $D_B = 3D_E$, $W_E = 3W_B$, $N_B = 10^{18}$ cm^{-3}, and $n_{iB}^2 = n_i^2$. What is β_F for (a) $N_E = 10^{19}$ cm^{-3}, (b) $N_E = 10^{20}$ cm^{-3}, and (c) $N_E = 10^{20}$ cm^{-3} and the base is substituted with SiGe with a band narrowing of $\Delta E_{gB} = 60$ meV?

SOLUTION:

a. At $N_E = 10^{19}$ cm^{-3}, $\Delta E_{gE} \approx$ 50 meV

$$n_{iE}^2 = n_i^2 e^{\Delta E_{gE}/kT} = n_i^2 e^{50/26\,\mathrm{meV}} = n_i^2 e^{1.92} = 6.8 n_i^2$$

From Eq. (8.4.5), $$\beta_F = \frac{D_B W_E}{D_E W_B} \times \frac{N_E n_i^2}{N_B n_{iE}^2} = \frac{9 \cdot 10^{19} \cdot n_i^2}{10^{18} \cdot 6.8 n_i^2} = 13$$

b. At $N_E = 10^{20}$ cm^{-3}, $\Delta E_{gE} \approx$ 95 meV

$$n_{iE}^2 = n_i^2 e^{\Delta E_{gE}/kT} = n_i^2 e^{95/26\,\mathrm{meV}} = n_i^2 e^{3.65} = 38 n_i^2$$

$$\beta_F = \frac{D_B W_E}{D_E W_B} \times \frac{N_E n_i^2}{N_B n_{iE}^2} = \frac{9 \cdot 10^{20} \cdot n_i^2}{10^{18} \cdot 38 n_i^2} = 24$$

Increasing N_E from 10^{19} cm^{-3} to 10^{20} cm^{-3} does not increase β_F by anywhere near 10 × because of band-gap narrowing. β_F can be raised of course by reducing N_B at the expense of a higher base resistance, which is detrimental to device speed (see Eq. 8.9.6).

c. $$n_{iB}^2 = n_i^2 e^{\Delta E_{gB}/kT} = n_i^2 e^{60/26\,\mathrm{meV}} = 10 n_i^2$$

$$\therefore \quad \beta_F = \frac{D_B W_E}{D_E W_B} = 9 \times \frac{N_E n_{iB}^2}{N_B n_{iE}^2} = \frac{9 \cdot 10^{20} \cdot 10 n_{iB}^2}{10^{18} \cdot 39 n_i^2} = 237$$

8.4.3 Poly-Silicon Emitter

Whether the base material is SiGe or plain Si, a high-performance BJT would have a relatively thick (>100 nm) layer of As doped N$^+$ poly-Si film in the emitter (as shown in Fig. 8–7). Arsenic is thermally driven into the "base" by ~20 nm and converts that single-crystalline layer into a part of the N$^+$ emitter. This way, β_F is larger due to the large W_E, mostly made of the N$^+$ poly-Si. This is the **poly-Silicon emitter** technology. The simpler alternative, a deeper implanted or diffused N$^+$ emitter without the poly-Si film, is known to produce a higher density of crystal defects in the thin base (causing excessive emitters to collector leakage current or even shorts in a small number of the BJTs).

8.4.4 Gummel Plot and β_F Fall-Off at High and Low I_C

High-speed circuits operate at high I_C, and low-power circuits may operate at low I_C. Current gain, β, drops at both high I_C and at low I_C. Let us examine the causes.

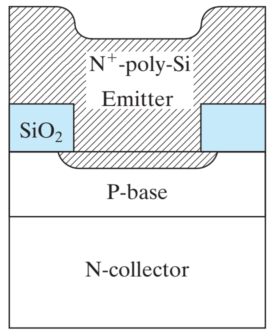

FIGURE 8–7 Schematic illustration of a poly-Si emitter, a common feature of high-performance BJTs.

We have seen in Fig. 8–5 (Gummel plot) that I_C flattens at high V_{BE} due to the high-level injection effect in the base. That I_C curve is replotted in Fig. 8–8. I_B, arising from hole injection into the emitter, does not flatten due to this effect (Fig. 8–8) because the emitter is very heavily doped, and it is practically impossible to inject a higher density of holes than N_E.

Over a wide mid-range of I_C in Fig. 8–8, I_C and I_B are parallel, indicating that the ratio of I_C/I_B, i.e., β_F, is a constant. This fact is obvious in Fig. 8–9. Above 1 mA, the slope of I_c in Fig. 8–8 drops due to high-level injection. Consequently, the I_c/I_B ratio or β_F decreases rapidly as shown in Fig. 8–9. This fall-off of current gain unfortunately degrades the performance of BJTs at high current where the BJT's speed is the highest (see Section 8.9). I_B in Fig. 8–8 is the base–emitter junction forward-bias current. As shown in Fig. 4–22, forward-bias current slope decreases at low V_{BE} or very low current due to the space-charge region (SCR) current (see Section 4.9.1). A similar slope change is sketched in Fig. 8–8. As a result, the I_c/I_B ratio or β_F decreases at very low I_C. The weak V_{BC} dependence of β_F in Fig. 8–9 is explained in the next section.

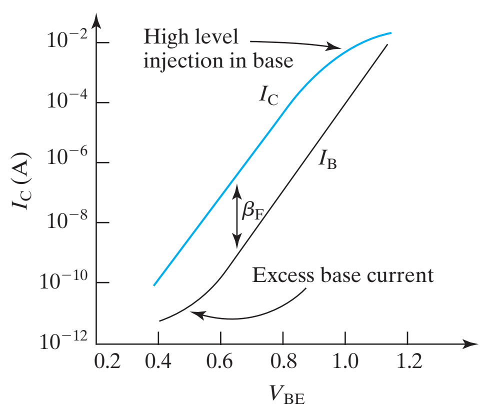

FIGURE 8–8 Gummel plot of I_C and I_B indicates that β_F (= I_C/I_B) decreases at high and low I_C.

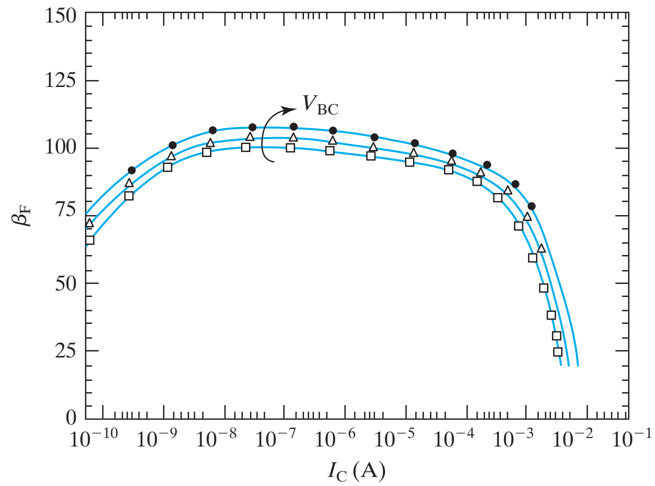

FIGURE 8–9 Fall-off of current gain at high- and low-current regions. $A_E = 0.6 \times 4.8\ \mu m^2$. From top to bottom: $V_{BC} = 2$, 1 and 0 V. Symbols are data. Lines are from a BJT model for circuit simulation. (From [3].)

8.5 ● BASE-WIDTH MODULATION BY COLLECTOR VOLTAGE ●

Instead of the flat I_C–V_{CE} characteristics shown in Fig. 8–2c, Fig. 8–10a (actual I_C – V_{CE} data) clearly indicates the presence of finite slopes. As in MOSFETs, a large **output conductance**, $\partial I_C/\partial V_{CE}$, of BJTs is deleterious to the voltage gain of circuits. The cause of the output conductance is **base-width modulation**, explained in Fig. 8–11. The thick vertical line indicates the location of the base-collector junction. With increasing V_{ce}, the base-collector depletion region widens and the neutral base width decreases. This leads to an increase in I_C as shown in Fig. 8–11.

If the $I_C - V_{CE}$ curves are extrapolated as shown in Fig. 8–10b, they intercept the $I_C = 0$ axis at approximately the same point. Figure 8–10b defines the **Early voltage**, V_A. V_A is a parameter that describes the flatness of the I_C curves. Specifically, the output resistance can be expressed as V_A/I_C:

$$r_0 \equiv \left(\frac{\partial I_C}{\partial V_{CE}}\right)^{-1} = \frac{V_A}{I_C} \tag{8.5.1}$$

A large V_A(i.e., a large r_0) is desirable for high voltage gains. A typical V_A is 50 V. V_A is sensitive to the transistor design. Qualitatively, we can expect V_A and r_0 to increase (i.e., expect the base-width modulation to be a smaller fraction of the base width) if we:

(a) increase the base width

(b) increase the base doping concentration, N_B, or

(c) decrease the collector doping concentration, N_C.

Clearly, (a) would reduce the sensitivity to any given ΔW_B (see Fig. 8–11). (b) would reduce the depletion region thickness on the base side because the depletion region penetrates less into the more heavily doped side of a PN junction

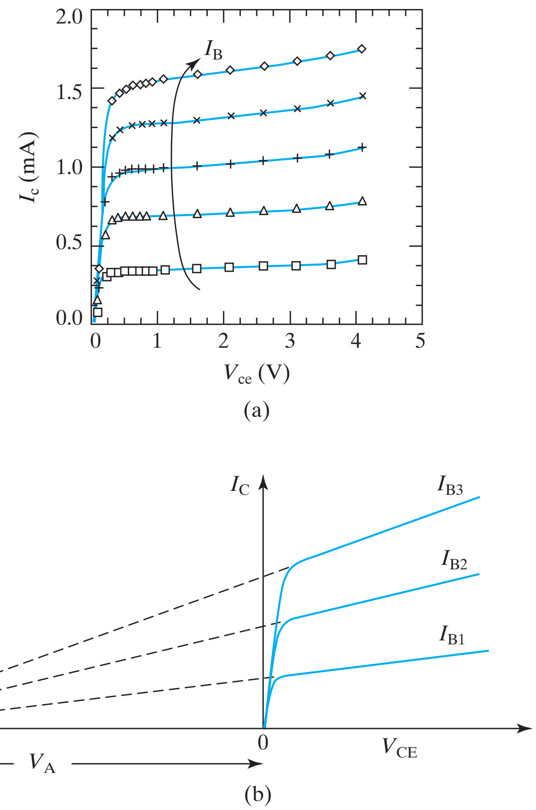

FIGURE 8–10 BJT output conductance: (a) measured BJT characteristics. I_B = 4, 8, 12, 16, and 20 μA. (From [3]); (b) schematic drawing illustrates the definition of Early voltage, V_A.

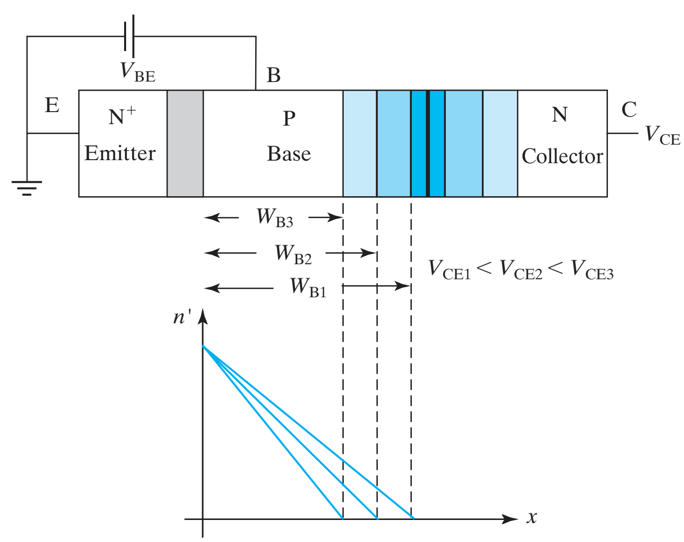

FIGURE 8–11 *As V_C increases, the BC depletion layer width increases and W_B decreases causing* dn'/dx *and I_C to increase.* In reality, the depletion layer in the collector is usually much wider than that in the base.

[see Eq. (4.2.5)]. For the same reason, (c) would tend to move the depletion region into the collector and thus reduce the depletion region thickness on the base side, too. Both (a) and (b) would depress β_F [see Eq. (8.4.5)]. (c) is the most acceptable course of action. It also reduces the base–collector junction capacitance, which is a good thing. Therefore, the collector doping is typically ten times lighter than base doping. In Fig. 8–10, the larger slopes at $V_{CE} > 3V$ are caused by impact ionization (Section 4.5.3). The rise of I_c due to base-width modulation is known as the **Early effect**, after its discoverer.

Early on Early Voltage

Anecdote contributed by Dr. James Early, November 10, 1990

"In January, 1952, on my way to a Murray Hill Bell Labs internal meeting, I started to think about how to model the collector current as a function of the collector voltage. Bored during the meeting, I put down the expression for collector current $I_C = \beta_F I_B$. Differentiating with respect to V_C while I_B was held constant gave:

$$\frac{\partial I_C}{\partial V_C} = I_B \frac{\partial \beta_F}{\partial V_C}$$

How can β_F change with V_C? Of course! The collector depletion layer thickens as collector voltage is raised. The base gets thinner and current gain rises. Obvious! And necessarily true.

Why wasn't this found sooner? Of those who had thought about it at all before, none was educated in engineering analysis of electron devices, used to setting up new models, and bored at a meeting."

8.6 • EBERS–MOLL MODEL •

So far, we have avoided examining the part of the I–V curves in Fig. 8–12 that is close to $V_{CE} = 0$. This portion of the I–V curves is known as the **saturation region** because the base is saturated with minority carriers injected from both the emitter and the collector. (Unfortunately the MOSFET saturation region is named in exactly the opposite manner.) The rest of the BJT operation region is known as the **active region** or the linear region because that is where BJT operates in active circuits such as the linear amplifiers.

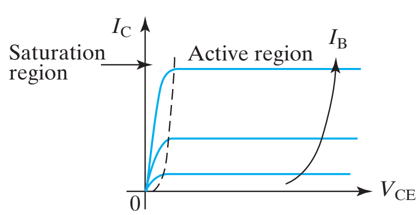

FIGURE 8–12 In the saturation region, I_C drops because the collector–base junction is significantly forward biased.

The Ebers–Moll model is a way to visualize as well as to mathematically describe both the active and the saturation regions of BJT operation. It is also the basis of BJT SPICE models for circuit simulation. The starting point is the idea that I_C is driven by two forces, V_{BE} and V_{BC}, as shown in Fig. 8–13. Let us first assume that a V_{BE} is present but $V_{BC} = 0$. Using Eq. (8.2.8),

$$I_C = I_S(e^{qV_{BE}/kT} - 1) \tag{8.6.1}$$

$$I_B = \frac{I_S}{\beta_F}(e^{qV_{BE}/kT} - 1) \tag{8.6.2}$$

Now assume that the roles of the collector and emitter are reversed, i.e., a (possibly forward bias) V_{BC} is present and $V_{BE} = 0$. Electrons would be injected from the collector into base and flow to the emitter. The collector now functions as the emitter and the emitter functions as the collector[4]

$$I_E = I_S(e^{qV_{BC}/kT} - 1) \tag{8.6.3}$$

$$I_B = \frac{I_S}{\beta_R}(e^{qV_{BC}/kT} - 1) \tag{8.6.4}$$

$$I_C = -I_E - I_B = -I_S\left(1 + \frac{1}{\beta_R}\right)(e^{qV_{BC}/kT} - 1) \tag{8.6.5}$$

β_R is the **reverse current gain**. (This is why β_F has F as the subscript. β_F is the **forward current gain**.) While β_F is usually quite large, β_R is small because the doping concentration of the collector, which acts as the "emitter" in the reverse mode, is not high. When both V_{BE} and V_{BC} are present, Eqs. (8.6.1) and (8.6.5) are superimposed as are Eqs. (8.6.2) and (8.6.4).

$$I_C = I_S(e^{qV_{BE}/kT} - 1) - I_S\left(1 + \frac{1}{\beta_R}\right)(e^{qV_{BC}/kT} - 1) \tag{8.6.6}$$

$$I_B = \frac{I_S}{\beta_F}(e^{qV_{BE}/kT} - 1) + \frac{I_S}{\beta_R}(e^{qV_{BC}/kT} - 1) \tag{8.6.7}$$

Equations (8.6.6) and (8.6.7) compromise the Ebers–Moll model as commonly used in SPICE models. These two equations can generate I_C vs. V_{CE} plots with excellent agreement with measured data as shown in Fig. 8–14.

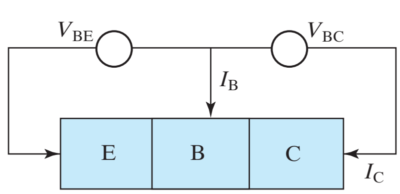

FIGURE 8–13 I_C is driven by two voltage sources, V_{BE} and V_{BC}.

[4] When the emitter and collector roles are interchanged, the upper and lower limits of integration in Eq. (8.2.11) are interchanged with no effect on G_B or I_S.

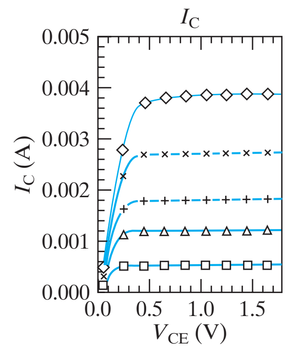

FIGURE 8–14 Ebers–Moll model (line) agrees with the measured data (symbols) in both the saturation and linear regions. I_B = 4.3, 11, 17, 28, and 43 µA. High-speed SiGe-base BJT. $A_E = 0.25 \times 5.75\ \mu m^2$. (From [3].)

What causes I_C to decrease at low V_{CE}? In this region, both the BE and BC junctions are forward biased. (For example: V_{BE} = 0.8 V, V_{BC} = 0.6 V, thus V_{CE} = 0.2 V.) A forward-biased V_{BC} causes the n' at $x = W_B$ to rise in Fig. 8–4. This depresses dn'/dx *and therefore I_C.*

8.7 • TRANSIT TIME AND CHARGE STORAGE •

Static IV characteristics are only one part of the BJT story. Another part is its dynamic behavior or its speed. When the BE junction is forward biased, excess holes are stored in the emitter, the base, and even the depletion layers. We call the sum of all the excess hole charges everywhere Q_F. Q_F is the stored **excess carrier charge**. If Q_F = 1 pC (pico coulomb), there is +1 pC of excess hole charge and –1 pC of excess electron charge stored in the BJT.[5] The ratio of Q_F to I_C is called the **forward transit time,** τ_F.

$$\boxed{\tau_F \equiv \frac{Q_F}{I_C}} \tag{8.7.1}$$

Equation (8.7.1) states the simple but important fact that I_C and Q_F are related by a constant ratio, τ_F. Some people find it more intuitive to think of τ_F as the **storage time**. In general, Q_F and therefore τ_F are very difficult to predict accurately for a complex device structure. However, τ_F can be measured experimentally (see Sec. 8.9) and once τ_F is determined for a given BJT, Eq. (8.7.1) becomes a powerful conceptual and mathematical tool giving Q_F as a function of I_C, and vice versa. τ_F *sets a high-frequency limit of BJT operation.*

8.7.1 Base Charge Storage and Base Transit Time

To get a sense of how device design affects the transit time, let us analyze the excess hole charge in the base, Q_{FB}, from which we will obtain the base transit time, τ_{FB}.

Q_{FB} is qA_E times the area under the line in Fig. 8–15.

[5] This results from Eq. (2.6.2), $n' = p'$.

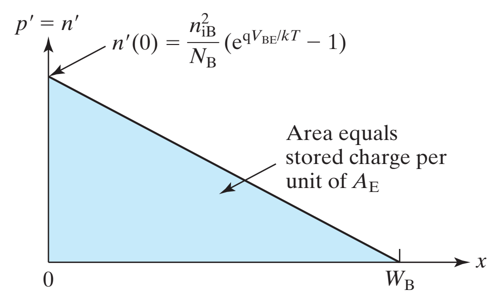

FIGURE 8–15 Excess hole and electron concentrations in the base. They are equal due to charge neutrality [Eq. (2.6.2)].

$$Q_{FB} = qA_E n'(0) W_B / 2 \tag{8.7.2}$$

Dividing Q_{FB} by I_C and using Eq. (8.2.7),

$$\boxed{\frac{Q_{FB}}{I_C} \equiv \tau_{FB} = \frac{W_B^2}{2D_B}} \tag{8.7.3}$$

To reduce τ_{FB} (i.e., to make a faster BJT), it is important to reduce W_B.

EXAMPLE 8–3 Base Transit Time

What is τ_{FB} if $W_B = 70$ nm and $D_B = 10\ \text{cm}^2/\text{s}$?

SOLUTION:

$$\tau_{FB} = \frac{W_B^2}{2D_B} = \frac{(7 \times 10^{-6}\text{cm})^2}{2 \times 10\ \text{cm}^2/\text{s}} = 2.5 \times 10^{-12}\text{s} = 2.5\ \text{ps}$$

2.5 ps is a very short time. Since light speed is 3×10^8 m/s, light travels less than 1 mm in 2.5 ps.

8.7.2 Drift Transistor–Built-In Base Field

The base transit time can be further reduced by building into the base a drift field that aids the flow of electrons from the emitter to the collector. There are two ways of accomplishing this. The classical method is to use graded base doping, i.e., a large N_B near the EB junction, which gradually decreases toward the CB junction as shown in Fig. 8–16a.

Such a doping gradient is automatically achieved if the base is produced by dopant diffusion. The changing N_B creates a dE_v/dx and a dE_c/dx. This means that there is a drift field [Eq. (2.4.2)]. Any electrons injected into the base would drift toward the collector with a base transit time shorter than the **diffusion transit time**, $W_B^2/2D_B$.

Figure 8–16b shows a more effective technique. In a **SiGe BJT**, P-type epitaxial $Si_{1-\eta}Ge_\eta$ is grown over the Si collector with a constant N_B and η linearly varying from about 0.2 at the collector end to 0 at the emitter end [4]. A large

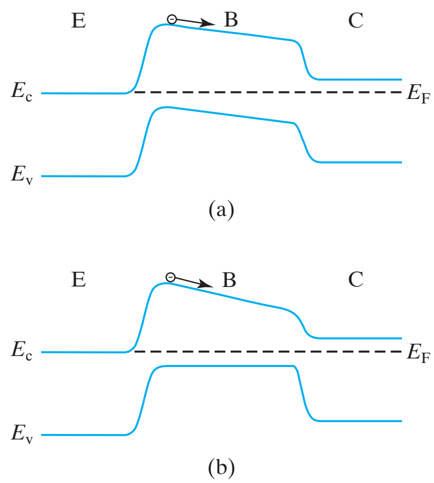

FIGURE 8–16 Two ways of building dE_C/dx into the base. (a) E_{gB} fixed, N_B decreasing from emitter end to collector end; (b) N_B fixed, E_{gB} decreasing from emitter end to collector end.

dE_c/dx can be produced by the grading of E_{gB}. These high-speed BJTs are used in high-frequency communication circuits. Drift transistors can have a base transit time several times less than $W_B^2/2D_B$, as short as 1 ps.

8.7.3 Emitter-to-Collector Transit Time and Kirk Effect[6]

The total forward transit time, τ_F, is also known as the **emitter-to-collector transit time**. τ_{FB} is only one portion of τ_F. The base transit time typically contributes about half of τ_F. To reduce the transit (or storage) time in the emitter and collector, the emitter and the depletion layers must be kept thin. τ_F can be measured, and an example of τ_F is shown in Fig. 8–17. τ_F starts to increase at a current density where the electron density corresponding to the dopant density in the collector ($n = N_C$) is insufficient to support the collector current even if the dopant-induced electrons move at the saturation velocity (see Section 6.8). This intriguing condition of too few dopant atoms and too much current leads to a reversal of the sign of the charge density in the "depletion region."

$$I_C = A_E q n v_{sat} \tag{8.7.4}$$

$$\begin{aligned} \rho &= qN_C - qn \\ &= qN_C - \frac{I_C}{A_E v_{sat}} \end{aligned} \tag{8.7.5}$$

$$\frac{d\mathscr{E}}{dx} = \rho/\varepsilon_s \tag{4.1.5}$$

[6] This section may be omitted in an accelerated course.

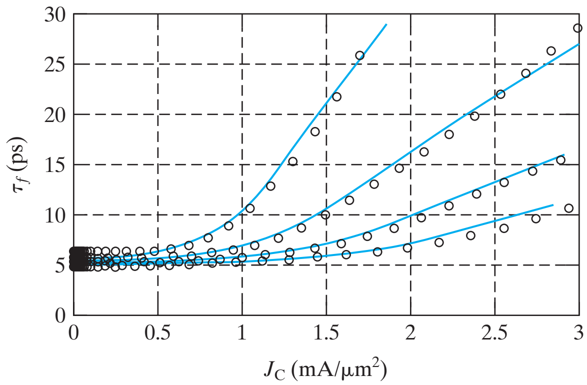

FIGURE 8–17 Transit time vs. I_C/A_E. From top to bottom: V_{CE} = 0.5, 0.8, 1.5, and 3 V. The rise at high I_C is due to base widening (Kirk effect). (From [3].)

When I_C is small, $\rho = qN_C$ as expected from the PN junction analysis (see Section 4.3), and the electric field in the depletion layer is shown in Fig. 8–18a. The shaded area is the potential across the junction, $V_{CB} + \phi_{bi}$. The N$^+$ collector is always present to reduce the series resistance (see Fig. 8–22). No depletion layer is

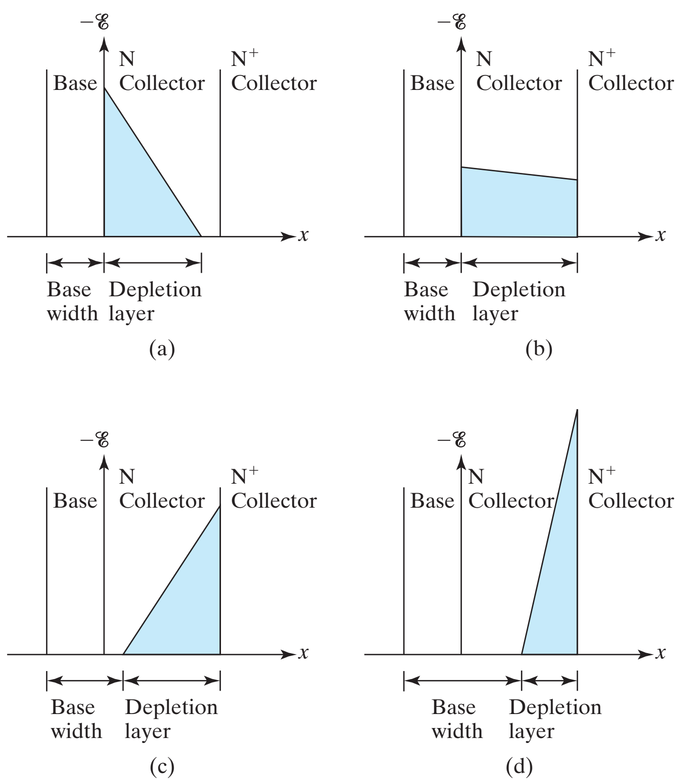

FIGURE 8–18 Electric field $\mathscr{E}(x)$, location of the depletion layer, and base width at (a) low I_C such as 0.1 mA/μm^2 in Fig. 8–17; (b) larger I_C; (c) even larger I_C (such as 1 mA/μm^2) and base widening is evident; and (d) very large I_C with severe base widening.

shown in the base for simplicity because the base is much more heavily doped than the collector. As I_C increases, ρ decreases [Eq. (8.7.5)] and $d\mathscr{E}/dx$ decreases as shown in Fig. 8–18b. The electric field drops to zero in the very heavily doped N^+ collector as expected. Note that the shaded area under the $\mathscr{E}(x)$ line is basically equal to the shaded area in the Fig. 8–18a because V_{CB} is kept constant. In Fig. 8–18c, I_C is even larger such that ρ in Eq. (8.7.5) and therefore $d\mathscr{E}/dx$ has changed sign. The size of the shaded areas again remains unchanged. In this case, the high-field region has moved to the right-hand side of the N collector. As a result, the base is effectively widened. In Fig. 8–18d, I_C is yet larger and the base become yet wider. Because of the **base widening**, τ_F increases as a consequence [see Eq. (8.7.3)]. This is called the **Kirk effect**. Base widening can be reduced by increasing N_C and V_{CE}. *The Kirk effect limits the peak BJT operating speed* (see Fig. 8–21).

8.8 ● SMALL-SIGNAL MODEL ●

Figure 8–19 is an equivalent circuit for the behavior of a BJT in response to a small input signal, e.g., a 10 mV sinusoidal signal, superimposed on the DC bias. BJTs are often operated in this manner in **analog circuits**.

If V_{BE} is not close to zero, the "1" in Eq. (8.2.8) is negligible; in that case

$$I_C = I_S e^{qV_{BE}/kT} \tag{8.8.1}$$

When a signal v_{BE} is applied to the BE junction, a collector current $g_m v_{BE}$ is produced. g_m, the **transconductance**, is

$$g_m \equiv \frac{dI_C}{dV_{BE}} = \frac{d}{dV_{BE}}(I_S e^{qV_{BE}/kT})$$

$$= \frac{q}{kT} I_S e^{qV_{BE}/kT} = I_C / \frac{kT}{q} \tag{8.8.2}$$

$$\boxed{g_m = I_C / \frac{kT}{q}} \tag{8.8.3}$$

At room temperature, for example, $g_m = I_C/26$ mV. The transconductance is determined by the collector bias current, I_C.

The input node, the base, appears to the input drive circuit as a parallel RC circuit as shown in Fig. 8–19.

$$\frac{1}{r_\pi} = \frac{dI_B}{dV_{BE}} = \frac{1}{\beta_F}\frac{dI_C}{dV_{BE}} = \frac{g_m}{\beta_F} \tag{8.8.4}$$

$$r_\pi = \beta_F / g_m \tag{8.8.5}$$

Q_F in Eq. (8.7.1) is the excess carrier charge stored in the BJT. If $Q_F = 1$ pC, there is +1 pC of excess holes and –1 pC of excess electrons in the BJT. All the excess hole charge, Q_F, is supplied by the base current, I_B. Therefore, the base presents this capacitance to the input drive circuit:

$$C_\pi = \frac{dQ_F}{dV_{BE}} = \frac{d}{dV_{BE}} \tau_F I_C = \tau_F g_m \tag{8.8.6}$$

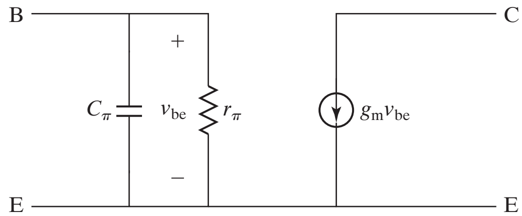

FIGURE 8–19 A basic small-signal model of the BJT.

The capacitance in Eq. (8.8.6) may be called the **charge-storage capacitance**, better known as the **diffusion capacitance**. In addition, there is one charge component that is not proportional to I_C and therefore cannot be included in Q_F [see Eq. (8.7.1)]. That is the junction depletion-layer charge. Therefore, a complete model of C_π should include the BE junction depletion-layer capacitance, C_{dBE}

$$C_\pi = \tau_F g_m + C_{dBE} \tag{8.8.7}$$

EXAMPLE 8–4 **Small-Signal Model Parameters**

The BJT represented in Figs. 8–9 and 8–17 is biased at I_C = 1 mA and V_{CE} = 3 V. T = 300 K and A_E = 5.6 μm². Find (a) g_m, (b) r_π, and (c) C_π.

SOLUTION:

a. $g_m \equiv I_C \Big/ \dfrac{kT}{q} = \dfrac{1\text{ mA}}{26\text{ mV}} = 39\dfrac{\text{mA}}{\text{V}} = 39\text{ mS (milli siemens)}$

b. From Fig. 8–9, $\beta_F = 90$ at I_C = 1 mA and V_{CB} = 2 V. ($V_{CB} = V_{CE} + V_{EB}$ = 3 V + $V_{EB} \approx$ 3 V −1 V = 2 V.)

$$r_\pi = \beta_F / g_m = \frac{90}{39\text{ mS}} = 2.3\text{ k}\Omega$$

c. From Fig. 8–17, at $J_C = I_C/A_E$ = 1 mA/5.6 μm² = 0.18 mA/μm² and V_{CE} = 3 V, we find τ_F = 5 ps.

$C_\pi = \tau_F g_m = 5 \times 10^{-12} \times 0.039 \approx 2.0 \times 10^{-13}$ F = 200 fF (femtofarad).

Once the parameters in Fig. 8–19 have been determined, one can use the small-signal model to analyze circuits with arbitrary signal-source impedance network (comprising resistors, capacitors, and inductors) and load impedance network as illustrated in Fig. 8–20a. The next section on cutoff frequency presents an example of the use of the small signal model.

While Fig. 8–20a is convenient for hand analysis, SPICE circuit simulation can easily use the more accurate small-signal model shown in Fig. 8–20b.

Some of the new parameters in Fig. 8–20b have familiar origins. For example, r_0 is the intrinsic output resistance, V_A/I_C (Section 8.5). C_μ also arises from base width modulation; when V_{BC} varies, the base width varies; therefore, the base stored charge (area of the triangle in Fig. 8–11) varies, thus giving rise to $C_\mu = dQ_{FB}/dV_{CB}$. C_{dBC} is the CB junction depletion-layer capacitance. Model

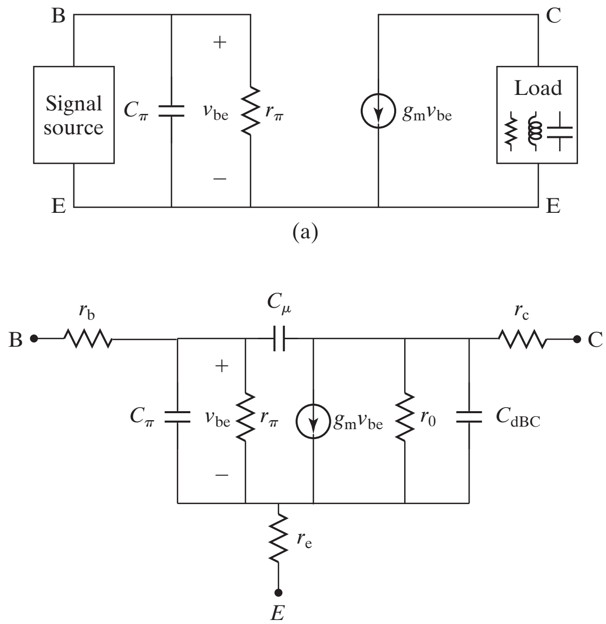

(b)

FIGURE 8–20 (a) The small-signal model can be used to analyze a BJT circuit by hand; (b) a small-signal model for circuit simulation by computer.

parameters are difficult to predict from theory with the accuracy required for commercial circuit design. Therefore, the parameters are routinely determined through comprehensive measurement of the BJT AC and DC characteristics.

8.9 ● CUTOFF FREQUENCY ●

Consider a special case of Fig. 8–20a. The load is a short circuit. The signal source is a current source, i_b, at a frequency f. At what frequency does the AC current gain $\beta\,(\equiv i_c/i_b)$ fall to unity?

$$v_{be} = \frac{i_b}{\text{input admittance}} = \frac{i_b}{1/r_\pi + j\omega C_\pi} \tag{8.9.1}$$

$$i_c = g_m v_{be} \tag{8.9.2}$$

Using Eqs. (8.9.1), (8.9.2), (8.8.7), and (8.8.3)

$$\beta(\omega) \equiv \left|\frac{i_c}{i_b}\right| = \frac{g_m}{|1/r_\pi + j\omega C_\pi|} = \frac{1}{|1/g_m r_\pi + j\omega\tau_F + j\omega C_{dBE}/g_m|}$$

$$= \frac{1}{|1/\beta_F + j\omega\tau_F + j\omega C_{dBE}kT/qI_C|} \tag{8.9.3}$$

At $\omega = 0$, i.e., DC, Eq. (8.9.3) reduces to β_F as expected. As ω increases, β drops. By carefully analyzing the $\beta(\omega)$ data, one can determine τ_F. If $\beta_F >> 1$ so that $1/\beta_F$ is negligible, Eq. (8.9.3) shows that $\beta(\omega) \propto 1/\omega$ and $\beta = 1$ at

$$f_T = \frac{1}{2\pi(\tau_F + C_{dBE}kT/qI_C)} \tag{8.9.4}$$

Using a more complete small-signal model similar to Fig. 8–20b, it can be shown that

$$f_T = \frac{1}{2\pi[\tau_F + (C_{dBE} + C_{dBC})kT/(qI_C) + C_{dBC}(r_e + r_c)]} \tag{8.9.5}$$

f_T is the cutoff frequency and is commonly used to compare the speed of transistors. Equations (8.9.4) and (8.9.5) predict that f_T rises with increasing I_C due to increasing g_m, in agreement with the measured f_T shown in Fig. 8–21. At very high I_C, τ_F increases due to base widening (Kirk Effect, Fig. 8–17), and therefore, f_T falls. *BJTs are often biased near the I_C where f_T peaks in order to obtain the best high-frequency performance.*

f_T is the frequency of **unity power gain**. The frequency of **unity power gain**, called the **maximum oscillation frequency**, can be shown to be [5]

$$f_{max} = \left(\frac{f_T}{8\pi r_b C_{dBC}}\right)^{1/2} \tag{8.9.6}$$

It is therefore important to reduce the base resistance, r_b.

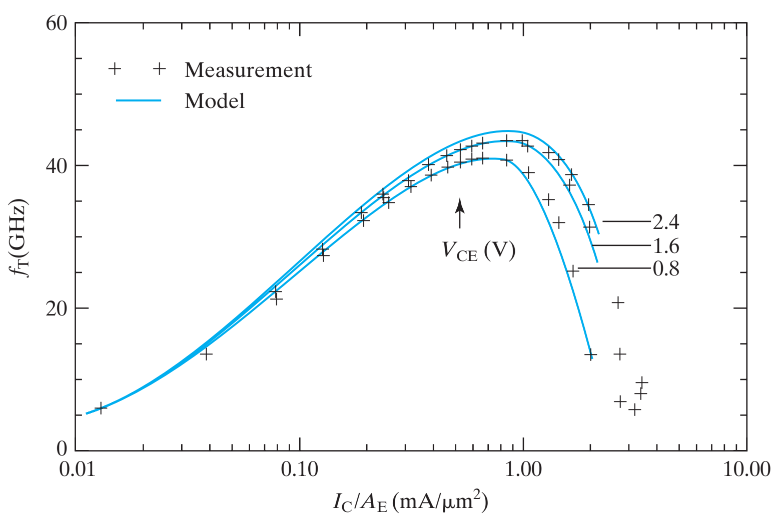

FIGURE 8–21 Cutoff frequency of a SiGe bipolar transistor. A compact BJT model matches the measured f_T well. (From [6]. © 1997 IEEE.)

BJT Structure for Minimum Parasitics and High Speed

While MOSFET scaling is motivated by the need for high packing density and large I_{dsat}, BJT scaling is often motivated by the need for high f_T and f_{max}. This involves the reduction of τ_F (thin base, etc.) and the reduction of parasitics (C_{dBE}, C_{dBC}, r_b, r_e, and r_c).

Figure 8–22 is a schematic of a high-speed BJT.

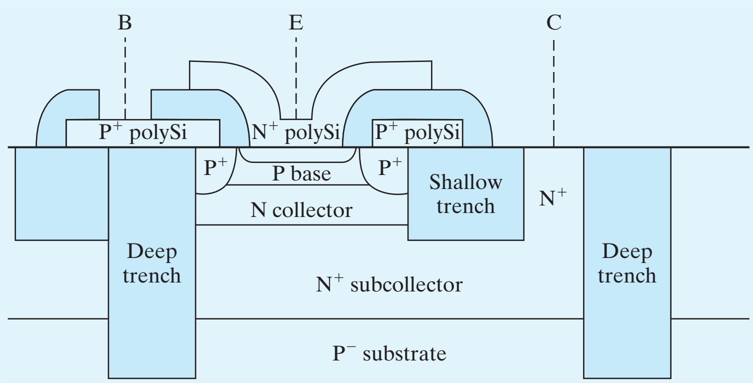

FIGURE 8–22 Schematic of a BJT with poly-Si emitter, self-aligned base, and deep-trench isolation. The darker areas represent electrical insulator regions.

An N^+ poly-Si emitter and a thin base are clearly seen in Fig. 8–22. The base is contacted through two small P^+ regions created by boron diffusion from a P^+ poly-Si film. The film also provides a low-resistance electrical connection to the base without introducing a large P^+ junction area and junction capacitance. To minimize the base series resistance, the emitter opening in Fig. 8–22 is made very narrow. The lightly doped epitaxial (see Section 3.7.3) N-type collector is contacted through a heavily doped subcollector in order to minimize the collector series resistance. The substrate is lightly doped to minimize the collector capacitance. Both the **shallow trench** and the **deep trench** are filled with dielectrics (SiO_2) and serve the function of electrical **isolation**. The deep trench forms a rectangular moat that completely surrounds the BJT. It isolates the collector of this transistor from the collectors of neighboring transistors. The structure in Fig. 8–22 incorporates many improvements that have been developed over the past decades and have greatly reduced the device size from older BJT designs. Still, a BJT is a larger transistor than a MOSFET.

8.10 • CHARGE CONTROL MODEL[7] •

The small-signal model is ideal for analyzing circuit response to small sinusoidal signals. What if the input signal is large? For example, what $I_C(t)$ is produced by a step-function I_B switching from zero to 20 μA or by any $I_B(t)$? The response can be

[7] This section may be omitted. Charge control model is used for analysis of digital switching operations.

conveniently analyzed with the **charge control model,** a simple extension of the charge storage concept (Eq. (8.7.1)).

$$I_C = Q_F/\tau_F \tag{8.10.1}$$

Assume that Eq. (8.10.1) holds true even if Q_F varies with time

$$\boxed{I_C(t) = Q_F(t)/\tau_F} \tag{8.10.2}$$

$I_C(t)$ becomes known if we can solve for $Q_F(t)$. (τ_F has to be characterized beforehand for the BJT being used.) Equation (8.10.2) suggests the concept that I_C is controlled by Q_F, hence the name of the charge control model. From Eq. (8.10.1), at DC condition,

$$I_B = I_C/\beta_F = Q_F/\tau_F\beta_F \tag{8.10.3}$$

Equation (8.10.3) has a straightforward physical meaning: *In order to sustain a constant excess hole charge in the transistor, holes must be supplied to the transistor through I_B to replenish the holes that are lost to recombination. Therefore, DC I_B is proportional to* Q_F. When holes are supplied by I_B at the rate of $Q_F/\tau_F\beta_F$, the rate of hole supply is exactly equal to the rate of hole loss to recombination and Q_F remains at a constant value. What if I_B is larger than $Q_F/\tau_F\beta_F$? In that case, holes flow into the BJT at a higher rate than the rate of hole loss–and the stored hole charge (Q_F) increases with time.

$$\boxed{\frac{dQ_F}{dt} = I_B(t) - \frac{Q_F}{\tau_F\beta_F}} \tag{8.10.4}$$

Equations (8.10.4) and (8.10.2), together constitute the basic charge control model. For any given $I_B(t)$, Eq. (8.10.4) can be solved for $Q_F(t)$ analytically or by numerical integration. Once $Q_F(t)$ is found, $I_C(t)$ becomes known from Eq. (8.10.2). We may interpret Eq. (8.10.4) with the analogy of filling a very leaky bucket from a faucet shown in Fig. 8–23. Q_F is the amount of water in the bucket, and $Q_F/\tau_F\beta_F$ is the rate

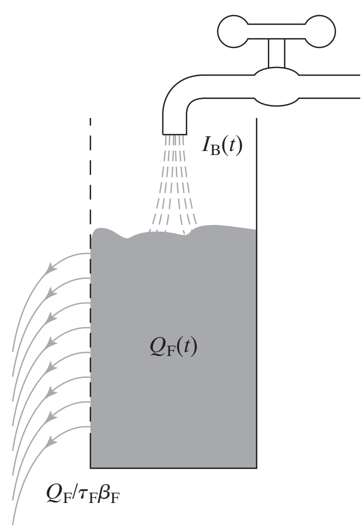

FIGURE 8–23 Water analogy of the charge control model. Excess hole charge (Q_F) rises (or falls) at the rate of supply (I_B) minus loss ($\propto Q_F$).

of water leakage. I_B is the rate of water flowing from the faucet into the bucket. If the faucet is turned fully open, the water level rises in the bucket; if it is turned down, the water level falls.

EXAMPLE 8–5 Finding $I_C(t)$ for a Step $I_B(t)$

QUESTION: τ_F and β_F of a BJT are given. $I_B(t)$ is a step function rising from zero to I_{B0} at $t = 0$ as shown in Fig. 8–24. Find $I_C(t)$.

SOLUTION:

At $t \geq 0$, $I_B(t) = I_{B0}$ and the solution of Eq. (8.10.4)

$$\frac{dQ_F}{dt} = I_B(t) - \frac{Q_F}{\tau_F \beta_F} \tag{8.10.4}$$

is

$$Q_F(t) = \tau_F \beta_F I_{B0}(1 - e^{-t/\tau_F \beta_F}) \tag{8.10.5}$$

Please verify that Eq. (8.10.5) is the correct solution by substituting it into Eq. (8.10.4). Also verify that the initial condition $Q_F(0) = 0$ is satisfied by Eq. (8.10.5). $I_C(t)$ follows Eq. (8.10.2).

$$I_C(t) = Q_F(t)/\tau_F = \beta_F I_{B0}(1 - e^{-t/\tau_F \beta_F}) \tag{8.10.6}$$

$I_C(t)$ is plotted in Fig. 8–24. At $t \to \infty$, $I_C = \beta_F I_{B0}$ as expected. $I_C(t)$ can be determined for any given $I_B(t)$ by numerically solving Eq. (8.10.4).

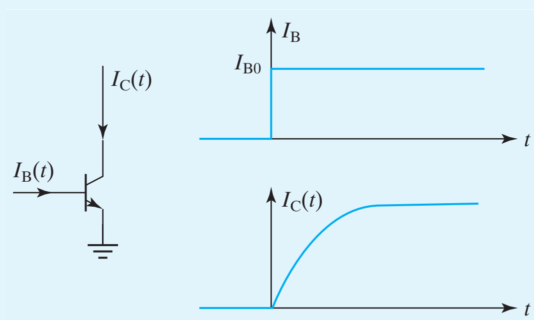

FIGURE 8–24 From the given step-function $I_B(t)$, charge control analysis can predict $I_C(t)$.

What we have studied in this section is a basic version of the charge control model. For a more exact analysis, one would introduce the junction depletion-layer capacitances into Eq. (8.10.4). Diverting part of I_B to charge the junction capacitances would produce an additional delay in $I_C(t)$.

8.11 • MODEL FOR LARGE-SIGNAL CIRCUIT SIMULATION •

The BJT model used in circuit simulators such as SPICE can accurately represent the DC and dynamic currents of the transistor in response to $V_{BE}(t)$ and $V_{CE}(t)$. A typical **circuit simulation model** or **compact model** is made of the Ebers–Moll model (with V_{BE} and V_{BC} as the two driving forces for I_C and I_B) plus additional enhancements for high-level injection, voltage-dependent capacitances that accurately represent the charge storage in the transistor, and parasitic resistances as shown in Fig. 8–25. This BJT model is known as the **Gummel–Poon model**.

The two diodes represent the two I_B terms due to V_{BE} and V_{BC} similar to Eq. (8.6.7). The capacitor labeled Q_F is voltage dependent such that the charge stored in it is equal to the Q_F described in Section 8.7. Q_R is the counterpart of Q_F produced by a forward bias at the BC junction. Inclusion of Q_R makes the dynamic response of the model accurate even when V_{BC} is sometimes forward biased. C_{BE} and C_{BC} are the junction depletion-layer capacitances. C_{CS} is the collector-to-substrate capacitance (see Fig. 8–22).

$$I_C = I_S'(e^{qV_{BE}/kT} - e^{qV_{BC}/kT})\left(1 + \frac{V_{CB}}{V_A}\right) - \frac{I_S}{\beta_R}(e^{qV_{BC}/kT} - 1) \qquad (8.11.1)$$

The similarity between Eqs. (8.11.1) and (8.6.6) is obvious. The $1 + V_{CB}/V_A$ factor is added to represent the Early effect—I_C increasing with increasing V_{CB}. I_S' differs from I_S in that I_S' decreases at high V_{BE} due to the high-level injection effect in accordance with Eq. (8.2.11) and as shown in Fig. 8–5.

$$I_B = \frac{I_S}{\beta_F}(e^{qV_{BE}/kT} - 1) + \frac{I_S}{\beta_R}(e^{qV_{BC}/kT} - 1) + I_{SE}(e^{qV_{BE}/n_E kT} - 1) \qquad (8.11.2)$$

Equation (8.11.2) is identical to Eq. (8.6.7) except for the additional third term, which represents the excess base junction current shown in Fig. 8–8. I_{SE} and n_E parameters are determined from the measured BJT data as are all of the several dozens of model parameters. The continuous curves in Figs. 8–9, 8–10a, and 8–17 are all examples of compact models. The excellent agreement between the models and the discrete data points in the same figures are necessary conditions for the

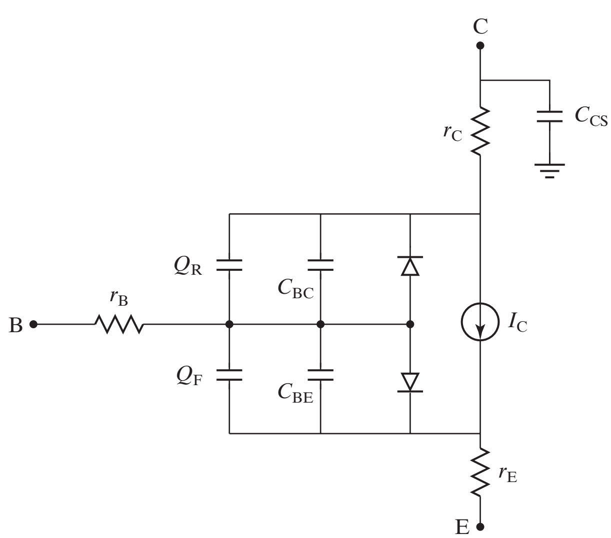

FIGURE 8–25 Illustration of a BJT model used for circuit simulation.

circuit simulation results to be accurate. The other necessary condition is that the capacitance in Fig. 8–24 be modeled accurately.

8.12 ● CHAPTER SUMMARY ●

The base–emitter junction is usually forward biased while the base–collector junction is reverse biased (as shown in Fig. 8–1b). V_{BE} determines the rate of electron injection from the emitter into the base, and thus uniquely determines the collector current, I_C, regardless of the reverse bias, V_{CB}

$$I_C = A_E \frac{qn_i^2}{G_B}(e^{qV_{BE}/kT} - 1) \qquad (8.2.9)$$

$$G_B \equiv \int_0^{W_B} \frac{n_i^2}{n_{iB}^2} \frac{p}{D_B} dx \qquad (8.2.11)$$

G_B is the base Gummel number, which represents all the subtleties of BJT design that affect I_C: base material, nonuniform base doping, nonuniform material composition, and the high-level injection effect.

An undesirable but unavoidable side effect of the application of V_{BE} is a hole current flowing from the base, mostly into the emitter. This base (input) current, I_B, is related to I_C by the common-emitter current gain, β_F.

$$\beta_F = \frac{I_C}{I_B} \approx \frac{G_E}{G_B} \qquad (8.4.1), (8.4.5)$$

where G_E is the emitter Gummel number. The common-base current gain is

$$\alpha_F \equiv \frac{I_C}{I_E} = \frac{\beta_F}{1 + \beta_F} \qquad (8.4.3)$$

The Gummel plot, Fig. 8–8, indicates that β_F falls off in the high I_C region due to high-level injection in the base and also in the low I_C region due to excess base current.

Base-width modulation by V_{CB} results in a significant slope of the I_C–V_{CE} curve in the active region. This is the Early effect. The slope, called the output conductance, limits the voltage gain that can be produced with a BJT. The Early effect can be suppressed with a lightly doped collector. A heavily doped subcollector (see Fig. 8–22) is routinely used to reduce the collector resistance.

Due to the forward bias, V_{BE}, a BJT stores a certain amount of excess hole charge, which is equal but of opposite sign to the excess electron charge. Its magnitude is called the excess carrier charge, Q_F. Q_F is linearly proportional to I_C.

$$Q_F \equiv I_C \tau_F \qquad (8.7.1)$$

τ_F is the forward transit time. If there were no excess carriers stored outside the base

$$\tau_F = \tau_{FB} = \frac{W_B^2}{2D_B} \qquad (8.7.3)$$

τ_{FB} is the base transit time. In general, $\tau_F > \tau_{FB}$ because excess carrier storage in the emitter and in the depletion layer are also significant. All these regions should be made small in order to minimize τ_F. Besides minimizing the base width, W_B, τ_{FB} may be reduced by building a drift field into the base with graded base doping (or better, with graded Ge content in a SiGe base). τ_{FB} is significantly increased at large I_C due to base widening, also known as the **Kirk effect**.

For computer simulation of circuits, the Gummel–Poon model, shown in Fig. 8–25, is widely used. Both the DC and the dynamic (charge storage) currents are well modeled. The Early effect and high-level injection effect are included. Simpler models consisting of R, C, and current source are used for hand analysis of circuits. The small-signal models (Figs. 8–19 and 8–20b) employ parameters such as transconductance

$$g_m \equiv \frac{dI_C}{dV_{BE}} = I_C / \frac{kT}{q} \tag{8.8.2}$$

input capacitance

$$C_\pi = \frac{dQ_F}{dV_{BE}} = \tau_F g_m \tag{8.8.6}$$

and input resistance.

$$r_\pi = \frac{dV_{BE}}{dI_B} = \beta_F / g_m \tag{8.8.5}$$

The BJT's unity-gain cutoff frequency (at which β falls to unity) is f_T. In order to raise device speed, device density, or current gain, a modern high-performance BJT usually employs (see Fig. 8–22) poly-Si emitter, self-aligned poly-Si base contacts, graded Si-Ge base, shallow oxide trench, and deep trench isolation. High-performance BJTs excel over MOSFETs in circuits requiring the highest device g_m and speed.

● PROBLEMS ●

● Energy Band Diagram of BJT ●

8.1 A Silicon PNP BJT with $N_{aE} = 5 \times 10^{18}$ cm^{-3}, $N_{dB} = 10^{17}$ cm^{-3}, $N_{aC} = 10^{15}$ cm^{-3}, and $W_B = 3$ μm is at equilibrium at room temperature.

(a) Sketch the energy band diagram for the device, properly positioning the Fermi level in the three regions.

(b) Sketch (i) the electrostatic potential, setting $V = 0$ in the emitter region, (ii) the electric field, and (iii) the charge density as a function of position inside the BJT.

(c) Calculate the net built-in potential between the collector and the emitter.

(d) Determine the quasi-neutral region width of the base.
Bias voltages of $V_{EB} = 0.6$ V and $V_{CB} = -2$ V are now applied to the BJT.

(e) Sketch the energy band diagram for the device, properly positioning the Fermi level in the three regions.

(f) On the sketches completed in part (b), sketch the electrostatic potential, electric field, and charge density as a function of position inside the biased BJT.

● IV Characteristics and Current Gain ●

8.2 Derive Eq. (8.4.4) from the definitions of β_F (Eq. 8.4.1) and α_F (Eq. 8.4.2).

8.3 Consider a conventional NPN BJT with uniform doping. The base–emitter junction is forward biased, and the base–collector junction is reverse biased.

- **(a)** Qualitatively sketch the energy band diagram.
- **(b)** Sketch the minority carrier concentrations in the base, emitter, and collector regions.
- **(c)** List all the causes contributing to the base and collector currents. You may neglect thermal recombination–generation currents in the depletion regions.

8.4 Neglect all the depletion region widths. The emitter, base, and collector of an NPN transistor have doping concentrations 10^{19}, 10^{17}, and 10^{15} cm^{-3} respectively. W_E = 0.8 μm, W_B = 0.5 μm, and W_C = 2.2 μm as shown in Fig. 8–26. Assume $\exp(qV_{BE}/kT) = 10^{10}$ and the base–collector junction is reverse biased. Assume that the device dimensions are much smaller than the carrier diffusion lengths throughout.

- **(a)** Find and plot the electron current density, $J_n(x)$, and hole current density, $J_p(x)$, in each region (J_p in the base is rather meaningless since it is three-dimensional in reality).
- **(b)** What are γ_E and β_F (assume L_B = 10 μm)?

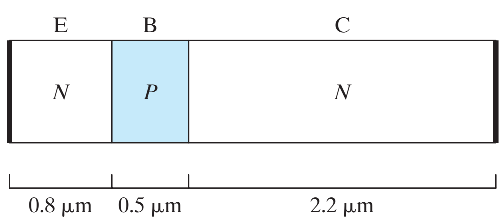

FIGURE 8–26

8.5 For the following questions, answer in one or two sentences.

- **(a)** Why should the emitter be doped more heavily than the base?
- **(b)** "The base width is small" is often stated in device analysis. What is it being compared with?
- **(c)** If the base width, W_B, were made smaller, explain how it would affect the base width modulation.
- **(d)** Why does β_F increase with increasing I_C at small values of collector current?
- **(e)** Explain why β_F falls off at large values of collector current.
- **(f)** For a PNP device, indicate the voltage polarity (+ or –) for the following:

Region of operation	V_{EB}	V_{CB}
Active		
Saturation		

● Schottky Emitter and Collector ●

8.6 The emitter of a high-β_F BJT should be heavily doped.

- **(a)** Is it desirable to replace the emitter in BJT with a metal?
- **(b)** Considering a metal on N–Si junction. The minority-carrier injection ratio is the number per second of minority carriers injected into the semiconductor divided by the majority carrier injected per second from the semiconductor into the metal when

the device is forward biased. The ratio is I_{diff} / I_{te}, where I_{diff} and I_{te} are respectively the hole diffusion current flowing into the semiconductor and the thermionic emission current of electrons flowing into the metal. Estimate the minority carrier injection ratio in an Si Schottky diode where K = 140 A/cm^{-2}, Φ_B = 0.72 eV, $N_d = 10^{16}$ cm^{-3}, $\tau_p = 10^{-6}$ s and T = 300 K. I_{diff} in the given diode is the same as the hole diffusion current into the N side of a P^+-N step junction diode with the same N_d & τ_p.

(c) If the collector in BJT is replaced with a metal, would it still function as a BJT? (Hint: Compare the energy diagrams of the two cases.)

● Gummel Plot ●

8.7 Consider an NPN transistor with $W_E = 0.5$ μm, $W_B = 0.2$ μm, $W_C = 2$ μm, $D_B = 10$ cm^2/s.

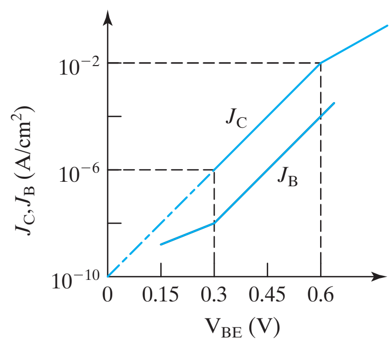

FIGURE 8–27

(a) Find the peak β_F from Fig. 8–27.

(b) Estimate the base doping concentration N_B.

(c) Find the V_{BE} at which the peak minority carrier concentration in the base is about to $N_B = 10^{17}$ cm^{-3}.

(d) Find the base transit time.

● Ebers–Moll Model ●

8.8 Consider the excess minority-carrier distribution of a PNP BJT as shown in Fig. 8–28. (The depletion regions at junctions are not shown.) Assume all generation–recombination current components are negligible and each region is uniformly doped. Constant $D_n = 30$ cm^2/s and $D_p = 10$ cm^2/s are given. This device has a cross-section area of 10^{-5} cm^2 and $N_E = 10^{18}$ cm^{-3}.

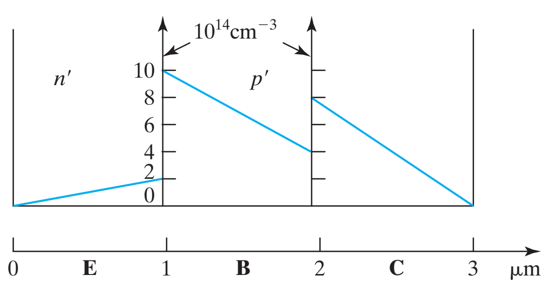

FIGURE 8–28

(a) Find N_C, i.e., the dopant concentration in the collector.

(b) In what region of the IV characteristics is this BJT operating? Explain your answer. (Hints: Are the BE and BE junctions forward or reverse biased?)

(c) Calculate the total stored excess carrier charge in the base (in Coulombs).

(d) Find the emitter current I_E.

(e) Calculate β_F, i.e., the common-emitter current gain when the BJT is operated in the nonsaturation region (i.e., V_{EB} >; 0.7 V and V_{CE} >; 0.3 V. Neglect base-width modulation).

8.9 An NPN BJT is biased so that its operating point lies at the boundary between active mode and saturation mode.

(a) Considering the Ebers–Moll of an NPN transistor, draw the simplified equivalent circuit for the transistor at the given operating point.

(b) Employing the simplified equivalent circuit of part (a), or working directly with Ebers–Moll equations, obtain an expression for V_{EC} at the specified operating point. Your answer should be in terms of I_B and the Ebers–Moll parameters.

● Drift-Base Transistors ●

8.10 An NPN BJT with a $Si_{0.8}Ge_{0.2}$ base has an E_{gB}, which is 0.1 eV smaller than an Si-base NPN BJT.

(a) At a given V_{BE}, how do I_B and I_C change when a SiGe base is used in place of an Si base? If there is a change, indicate whether the currents are larger or smaller.

(b) To reduce the base transit time and increase β, the percentage of Ge in an $Si_{1-x}Ge_x$ base is commonly graded in order to create a drift field for electrons across the base. Assume that E_g is linearly graded and that $x = 0$ at the emitter–base junction and x = 0.2 μm at the base–collector junction. What is $\beta(\text{SiGe})/\beta(\text{Si})$? (Hint: $n_{iB}^2 = n_{i,Si}^2 \exp[(\Delta E_{g,Si0.8Ge0.2}/kT)\,(x/W_B)]$, where W_B is the base width.)

8.11 An NPN transistor is fabricated such that the collector has a uniform doping of 5×10^{15} cm^{-3}. The emitter and base doping profiles are given by $N_{dE} = 10^{20}e(-x/0.106)$ cm^{-3}. And $N_{aB} = 4 \times 10^{18}(-x/0.19)$ cm^{-3}, where x is in micrometers.

(a) Find the intercept of N_{dE} and N_{aB} and the intercept of N_{aB} and N_c. What is the difference between the two intercepts? What is the base width ignoring the depletion widths, known as the **metallurgical base width**?

(b) Find base and emitter Gummel numbers. Ignore the depletion widths for simplicity.

(c) Find the emitter injection efficiency γ_E.

(d) Now considering only the N_{aB} doping in the base (ignore the other doping), sketch the energy band diagram of the base and calculate the built-in electric field, defined as $\mathscr{E}_{bi} = (1/q)(dE_c/dx)$, where E_c is the conduction band level.

● Kirk Effect ●

8.12 Derive an expression for the "base width" in Fig. 8–18c or Fig. 8–18d as a function of I_C, V_{CB}, and N-collector width, W_C. Assume all common BJT parameters are known.

● Charge Control Model ●

8.13 Solve the problem for the step-function I_B in Example 8–5 in Section 8.10 on your own without copying the provided solution.

8.14 A step change in base current occurs as shown in Fig. 8–29. Assuming forward active operation, estimate the collector current $i_C(t)$ for all time by application of the charge control model and reasonable approximations. Depletion region capacitance can be neglected. The following parameters are given: $\alpha_F = 0.9901$, $\tau_F = 10$ ps, $i_{B1} = 100$ μA, and $i_{B2} = 10$ μA.

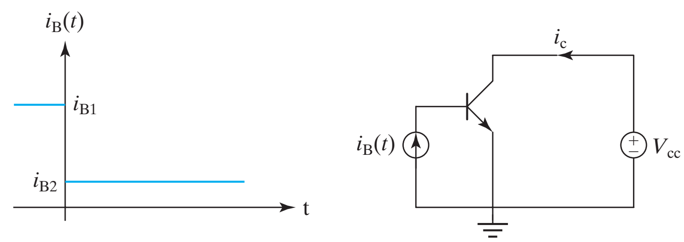

FIGURE 8–29

Cutoff Frequency

8.15 After studying Section 8.9, derive expressions for $\beta(\omega)$ and f_T.

REFERENCES

1. Taur, Y., and T. Ning. *Fundamentals of VLSI Devices.* Cambridge, UK: Cambridge University Press, 1998, Ch. 6.
2. del Alamo, J., S. Swirhum, and R. M. Swanson. "Simultaneous Measurement of Hole Lifetime, Mobility, and Bandgap Narrowing in Heavily Doped N-type Silicon." *International Electron Devices Meeting Technical Digest*. (1985), 290–293.
3. Paasschens, J., W. Kloosterman, and D.B.M. Klaassen. "Mextram 504." Presentation at Compact Model Council, September 29, 1999. http://www.eigroup.org/cmc/minutes/wk092999.pdf
4. Harame, D. L., et al. "Si/SiGe Epitaxial-Base Transistors." *IEEE Transactions on Electron Devices*, 42, 3 (1995), 455–482.
5. Roulston, D. J. *Bipolar Semiconductor Devices.* New York: McGraw Hill, 1990.
6. Tran, H. Q., et al. "Simultaneous Extraction of Thermal and Emitter Series-Resistances in Bipolar Transistors." Proceedings of the IEEE Bipolar/BiCMOS Circuits and Technology Meeting, Minneapolis, MN, 1997.

GENERAL REFERENCES

1. Roulston, D. J. *Bipolar Semiconductor Devices.* New York: McGraw-Hill, 1990.
2. Taur, Y., and T. Ning. *Fundamentals of VLSI Devices.* Cambridge, UK: Cambridge University Press, 1998.